Neuroradiology (2023) 65:361–370
https://doi.org/10.1007/s00234-022-03067-9

FUNCTIONAL NEURORADIOLOGY

Disrupted topological organization of resting-state functional brain networks in Parkinson's disease patients with glucocerebrosidase gene mutations

Yanbing Hou[1] · Fei Feng[1] · Lingyu Zhang[1] · Ruwei Ou[1] · Junyu Lin[1] · Qiyong Gong[2] · Huifang Shang[1]

Received: 29 June 2022 / Accepted: 11 October 2022 / Published online: 21 October 2022

Abstract

Purpose The mutations of the glucocerebrosidase (GBA) gene are the greatest genetic risk factor for Parkinson's disease (PD). The mechanism underlying the association between GBA mutations and PD has not been fully elucidated.

Methods Using resting-state functional magnetic resonance imaging and graph theory analysis to investigate the disrupted topological organization in PD patients with GBA mutation (GBA-PD). Eleven GBA-PD patients, 11 noncarriers with PD, and 18 healthy controls (HCs) with a similar age and sex distribution were recruited. Individual whole-brain functional connectome was constructed, and the global and nodal topological disruptions were calculated among groups. Partial correlation analyses between the clinical features of patients with PD and topological alterations were performed.

Results The GBA-PD group showed prominently decreased characteristic path length (L_p) and increased global efficiency (E_g) compared to HCs at the global level; a significantly increased nodal betweenness centrality in the medial prefrontal cortex (mPFC) and precuneus within the default mode network, and precentral gyrus within the sensorimotor network, while a significantly decreased betweenness centrality in nodes within the cingulo-opercular network compared to the noncarrier group at the regional level. The altered nodal betweenness centrality of mPFC was positively correlated with fatigue severity scale scores in all patients with PD.

Conclusion The preliminary pilot study found that GBA-PD patients had a higher functional integration at the global level. The nodal result of the mPFC is congruent with the potential fatigue pathology in PD and is suggestive of a profound effect of GBA mutations on the clinical fatigue in patients with PD.

Keywords Glucocerebrosidase gene · Parkinson's disease · Graph theory · Resting-state functional magnetic resonance imaging · Fatigue

✉ Qiyong Gong
huaxigongqy@163.com

✉ Huifang Shang
hfshang2002@126.com

Yanbing Hou
ybhou2019@126.com; 123301023@qq.com

Fei Feng
bruisefei@163.com

Lingyu Zhang
lyzhang2016120@163.com

Ruwei Ou
ouruwei@aliyun.com

Junyu Lin
ouruwei@aliyun.com

[1] Department of Neurology, Laboratory of Neurodegenerative Disorders, National Clinical Research Center for Geriatrics, West China Hospital, Sichuan University, Chengdu 610041, Sichuan, China

[2] Huaxi MR Research Center (HMRRC), Department of Radiology, West China Hospital, Sichuan University, Chengdu 610041, Sichuan, China

Introduction

Parkinson's disease (PD) is the most common neurodegenerative movement disorder with a broad range of causes and clinical presentations [1]. Genetics, environment, and interactions thereof are major factors related to the causes of PD. In the past 20 years, more than 27 genes have been confirmed to be related to parkinsonism, and mutations in the glucocerebrosidase (GBA) gene that encodes the lysosomal glucocerebrosidase (GCase) have been found to constitute the greatest risk factor for sporadic PD [2]. More than 300 mutations in GBA have been reported. However, to date, the mechanism leading to the increased risk of PD in GBA mutation carriers is multifaceted (e.g., α-synuclein aggregation, endoplasmic reticulum stress, and disturbances of lysosomal-autophagy [3]) and has not been fully elucidated.

Numerous studies have revealed the clinical characteristics of PD patients with GBA variants (GBA-PD). Compared with noncarriers with PD, GBA-PD patients are associated with an earlier age at onset and an increased risk of mortality [4]. Despite that GBA-PD does not present clinical features that can be distinguished from idiopathic PD (iPD), it is recognized that GBA mutation carriers have a more aggressive disease course [4], including several motor features (e.g., more symmetrical symptoms, the faster progression of motor disability, and higher prevalence of disabling motor features such as freezing of gait), and the higher risk for developing some non-motor symptoms (e.g., dementia, neuropsychiatric disturbances, autonomic dysfunction, and sleep disturbances). Considering the potential relevance of GBA to disease prognosis and new therapeutic approaches, the search for GBA-PD-related biomarkers has become crucial.

Conventional magnetic resonance imaging (MRI) techniques have been used to support the diagnosis of PD in clinical practice, and the advanced imaging techniques (e.g., structural MRI and resting-state functional MRI (rs-fMRI)) are applied to clarify the pathophysiology of the disease and provide information on the underlying neurodegenerative processes [5]. In the past years, several neuroimaging studies have focused on GBA-PD patients to elucidate the pathophysiology in GBA-PD populations [6]. Compared to iPD and healthy controls (HCs), GBA-PD patients showed a left-sided prevalent pattern of cortical thinning involving parietal, temporal, and occipital regions at baseline, and a greater pattern of cortical thinning of posterior and frontal regions after 5-year follow-up of this cohort [7], which supported the hypothesis that GBA mutations are involved in accelerating the neurodegenerative process of PD. Conversely, the other two studies assessing the pattern of gray matter (GM) atrophy did not report any differences in the GM volume between GBA-PD and iPD patients [8, 9]. Only one rs-fMRI study analyzing the seed-to-voxel functional connectivity of putamen, caudate, and nucleus accumbens showed that the reduced connectivity in the parieto-occipital regions in the GBA-PD group relative to the iPD group [10], which revealed changes in cortico-subcortical functional networks.

In recent years, graph theory analysis has attracted extensive attention in the neuroimaging analysis fields, which can be used to investigate the topological organization of brain networks, and offer important insights into the potential mechanism of disease. Different from the seed-based analysis, the graph theory analysis that can construct a strong framework for describing the abnormal brain connectome has been widely used to explore the pathophysiological changes in psychiatric and neurological diseases, including PD. For instance, one of our previous studies showed a disruption of whole-brain topological organization in early-stage drug-naïve patients with PD, contributing to the preclinical changes of the cognitive process in patients with PD [11]. To our knowledge, no graph theory study has separated GBA-PD patients from those noncarriers with PD.

In the current study, we wished to investigate the topological organization of whole-brain functional networks in GBA-PD patients compared with HCs and noncarriers with PD in order to understand the in vivo topological correlates of GBA mutations in PD, and whether topological changes would significantly correlate with the clinical characteristics of patients with PD.

Patients and methods

Approval was received from the West China Hospital of Sichuan University Clinical trials and Biomedical ethics committee, and written informed consent was obtained from all participants in the study.

Participants

Patients with PD diagnosed according to the UK PD Brain Bank criteria [12] were recruited at the Department of Neurology of West China Hospital of Sichuan University. Patients with PD in the study underwent an extensive study protocol with the assessment of motor and non-motor symptoms, neuroimaging, and genetic analysis. Patients were excluded if they had (1) left-handedness; (2) moderate to severe head tremor at rest; (3) PD dementia according to the Movement Disorder Society (MDS) diagnostic criteria [13]; (4) a history of cerebrovascular disorders, brain injury, neurological surgery, and any other neurological conditions; (5) structural brain defects on T1- or T2 weighted imaging (i.e., being abnormal on conventional MRI). The presence of

GBA mutations (rare pathogenic/likely pathogenic variants) in 11 patients with PD (refer to Supplementary Table S1 for specific mutations and types) and 11 noncarriers with PD without rare variants in PD genes (e.g., *GBA*, *LRRK2*, *SNCA*, *PRKN*, *PARK7*, *PINK1*, *VPS35*) matched for age, sex, education, disease duration, levodopa equivalent daily dose (LEDD), and disease severity were enrolled (Table 1). In addition, 18 HCs with a similar age and sex distribution were recruited. These control subjects (1) had no history of neurologic, psychiatric, or other disorders; (2) were normal on conventional MRI.

The demographic and clinical data were collected using a standard questionnaire by an experienced neuropsychologist who was blinded to GBA status of patients with PD. The patients were either drug-naïve at the initial visit or in an OFF state (un-medicated for at least 12 h before participation). Handedness, age, sex, education, disease duration, and LEDD [14] were collected. The unified PD rating scale (UPDRS) was used to evaluate non-motor symptoms (Part I), motor symptoms (Part II), and motor signs (Part III). The disease stage was defined by the Hoehn and Yahr (H&Y) stage. The non-motor symptoms were assessed using the non-motor symptoms scale (NMSS) (9 domains). The executive function was evaluated using the frontal assessment battery (FAB), and the global cognitive function was evaluated using the Montreal cognitive assessment (MoCA). The Hamilton depression rating scale (HDRS) containing 24 items and the Hamilton anxiety rating scale (HARS) were used to evaluate depression and anxiety symptoms, respectively. The fatigue severity scale containing 9 items was used to measure the severity of fatigue. Each patient can be categorized into two groups: the absence of fatigue (fatigue severity scale total score ≤ 36) or the presence of fatigue (fatigue severity scale total score > 36). The PD sleep scale (PDSS) and rapid eye movement sleep behavior disorder screening questionnaire (RBDSQ, 13 items) were used to quantify sleep problems. The PD questionnaire 39 (PDQ-39) was used to evaluate the quality of life of PD patients.

Table 1 Demographic and clinical characteristics of PD patients and healthy controls

Parameter	PD patients, all	Healthy controls	GBA-PD patients	Noncarriers with PD	*p*-value (ANOVA)	GBA-PD patients vs. noncarriers with PD
Number, *n*	22	18	11	11	-	-
Handedness (r: l)	22: 0	18: 0	11: 0	11: 0	-	-
Sex, m/f	12: 10	8: 10	5: 6	7: 4	0.568	-
Age, years	47.12 ± 7.42	49.87 ± 7.09	46.29 ± 8.16	47.94 ± 6.90	0.442	-
Education, years	-	-	8.91 ± 2.84	10.55 ± 3.27	-	0.225
Duration of disease, years	-	-	3.91 ± 2.85	2.55 ± 1.32	-	0.172
LEDD	-	-	276.14 ± 272.06	281.82 ± 196.56	-	0.789[#]
UPDRS score	-	-	-	-	-	
Part I	-	-	2.46 ± 2.42	1.00 ± 1.10	-	0.145[#]
Part II	-	-	10.18 ± 4.33	7.27 ± 3.61	-	0.102
Part III	-	-	31.09 ± 11.61	27.36 ± 10.21	-	0.357[#]
H & Y stage	-	-	2.05 ± 0.27	2.00 ± 0.00	-	0.545[#]
NMSS score	-	-	24.91 ± 32.81	18.73 ± 6.54	-	0.717[#]
FAB score	-	-	17.09 ± 1.45	16.55 ± 1.44	-	0.223[#]
MoCA score	-	-	26.46 ± 4.48	27.18 ± 2.18	-	0.815[#]
HDRS score	-	-	9.91 ± 9.60	8.55 ± 8.57	-	0.792
HARS score	-	-	7.55 ± 7.76	6.46 ± 6.35	-	0.722
FSS total score	-	-	36.64 ± 17.58	22.73 ± 15.28	-	0.062
Fatigue, yes/no	-	-	5/6	2/9		0.170
PDSS score	-	-	8.09 ± 7.62	8.46 ± 6.70	-	0.907
RBDSQ score	-	-	3.27 ± 2.41	2.27 ± 1.68	-	0.222[#]
PDQ-39 score	-	-	35.55 ± 29.67	22.18 ± 15.73	-	0.202
FD (power)	-	0.23 ± 0.12	0.23 ± 0.11	0.17 ± 0.06	0.349	-

ANOVA analysis of variance, *F* female, *FAB* frontal assessment battery, *FD* frame-wise displacement, *FSS* fatigue severity scale, *GBA* glucocerebrosidase gene, *H & Y* Hoehn & Yahr, *HARS* Hamilton anxiety rating scale, *HDRS* Hamilton depression rating scale, *L* left, *LEDD* levodopa equivalent daily dose, *M* male, *MoCA* Montreal cognitive assessment, *NMS* non-motor symptoms, *PD* Parkinson's disease *PDQ-39* Parkinson's disease questionnaire 39, *PDSS* Parkinson's disease sleep scale, *R* right, *RBDSQ* rapid eye movement sleep behavior disorder screening questionnaire, *UPDRS* unified Parkinson's disease rating scale

[#]Indicates the nonparametric test because of the non-normal distribution

MRI acquisition and preprocessing

MRI scanning was performed on a 3-Tesla MR scanner (Siemens, Trio Tim, Germany) with an eight-channel phased-array head coil. Before the scan, the respiration and heart rate of all participants remained normal. All participants were asked to remain awake and breathe quietly until the end of the scan. The rs-fMRI data were obtained through a gradient-echo echo-planar imaging (GE-EPI) sequence: repetition time/echo time $TR/TE = 2000/30$ ms, flip-angle $FA = 90°$, field of view $FOV = 240 \times 240$ mm^2, matrix size $= 64 \times 64$, voxel size $= 3.75 \times 3.75 \times 5$ mm^3, slice thickness $= 5.0$ mm (no slice gap). Each brain volume comprised 30 axial slices, and each functional run contained 240 image volumes.

Rs-fMRI data reprocessing was performed using the SPM12 (Statistical Parametric Mapping, http://www.fil.ion.ucl.ac.uk/spm) and DPABI (Data Processing & Analysis for Brain Imaging, http://rfmri.org/DPABI). The steps included: removing the first 10 image volumes of functional images, slice timing corrections, spatial realignment, spatial normalization into the standard Montreal neurological institute (MNI) space, resampling into $3 \times 3 \times 3$ mm^3 voxels, detrending, nuisance signal regression (including the Friston 24-parameters, white matter and cerebrospinal fluid signals), band-pass filtering (0.01–0.08 Hz), and scrubbing (frame-wise displacement (FD) threshold = 0.5 [15]; before poor quality frame time point number = 1; after poor quality frame time point number = 2). All participants had less than 1.5 mm maximum displacement in the *x*-, *y*-, or *z*-plane, and less than 1.5° angular rotation about each axis.

Network construction and topological analysis

A region-based functional connectivity network was constructed as described in our previous study [16], and graph theory analysis was used to analyze the brain network [17]. Briefly, a total of 160 regions of interest (ROIs) were identified by Dosenbach et al. (Supplementary Table S2) [18]. All voxels within each ROI were extracted to obtain the average time series, and the Pearson correlation of the mean time series between any two ROIs was calculated. Therefore, a 160×160 correlation matrix was computed for each participant. The topological properties of functional networks were investigated through the toolbox of GRETNA v2.0 (http://www.nitrc.org/projects/gretna/). To exclude the bias of a single sparse threshold, the correlation matrix for each participant was thresholded using the same sparsity ranging from 10 to 34% with an interval of 1% as our previous study [16], and the area under the curve (AUC) over sparsity ranges was calculated. Both global and regional measures of network topology were calculated, including (1) small-world parameters (clustering coefficient (C_p), characteristic path length (L_p), normalized C_p (γ), normalized L_p (λ), and small-worldness ($\sigma = \gamma/\lambda$)) and two network efficiency metrics (global efficiency (E_{glob}) and local efficiency (E_{loc})); (2) the regional measure (nodal betweenness centrality (BC)) (refer to Supplementary Table S3 for the general descriptions). More specifically, the term "small-world" organization commonly reflects an optimal balance of functional segregation and integration, and the "small-world'" network should be simultaneously highly segregated and integrated. The clustering coefficient and local efficiency are commonly used to measure the functional segregation; the characteristic path length and global efficiency are commonly used to measure the functional integration. In addition, nodal betweenness centrality is a measure of centrality that can act as the important control of information flow [19].

Statistical analysis

The chi-square test was used to analyze the sex ratios among the three groups, with the one-way analysis of variance (ANOVA) used for age and mean FD parameters. The student's *t*-test, chi-square test, or nonparametric test was used to detect differences of clinical data between two PD subgroups, as appropriate. To assess the significant differences in the topological properties, ANOVA was performed to compare the AUC value of each network metric among the three groups, and a pairwise post hoc test via the least-significant difference (LSD) method was subsequently used to identify significant inter-group differences. Furthermore, partial correlation analyses were used to assess the correlations between the above significant inter-group differences and clinical parameters in PD groups, with age, sex, education, LEDD, and mean FD as covariates. Since these analyses were exploratory in nature, $P < 0.05$ was considered significant.

Results

Demographic and clinical characteristics

Patients and HCs were similar with respect to their age, sex, and mean FD values. Patient subgroups were comparable for all clinical features. Notably, the GBA-PD group had relatively severer non-motor symptoms than the noncarrier group, especially in fatigue. Fatigue was found in 5 cases (45.45%) of the GBA-PD group, and 2 cases (18.18%) of the noncarrier group (Table 1).

Alterations in the topological properties

Over the sparsity range of 0.10–0.34 (step = 0.01), all participants showed the small-world properties ($\gamma > 1$, $\lambda \approx 1$, and $\sigma > 1$) (Fig. 1a). The GBA-PD patients, noncarriers with PD,

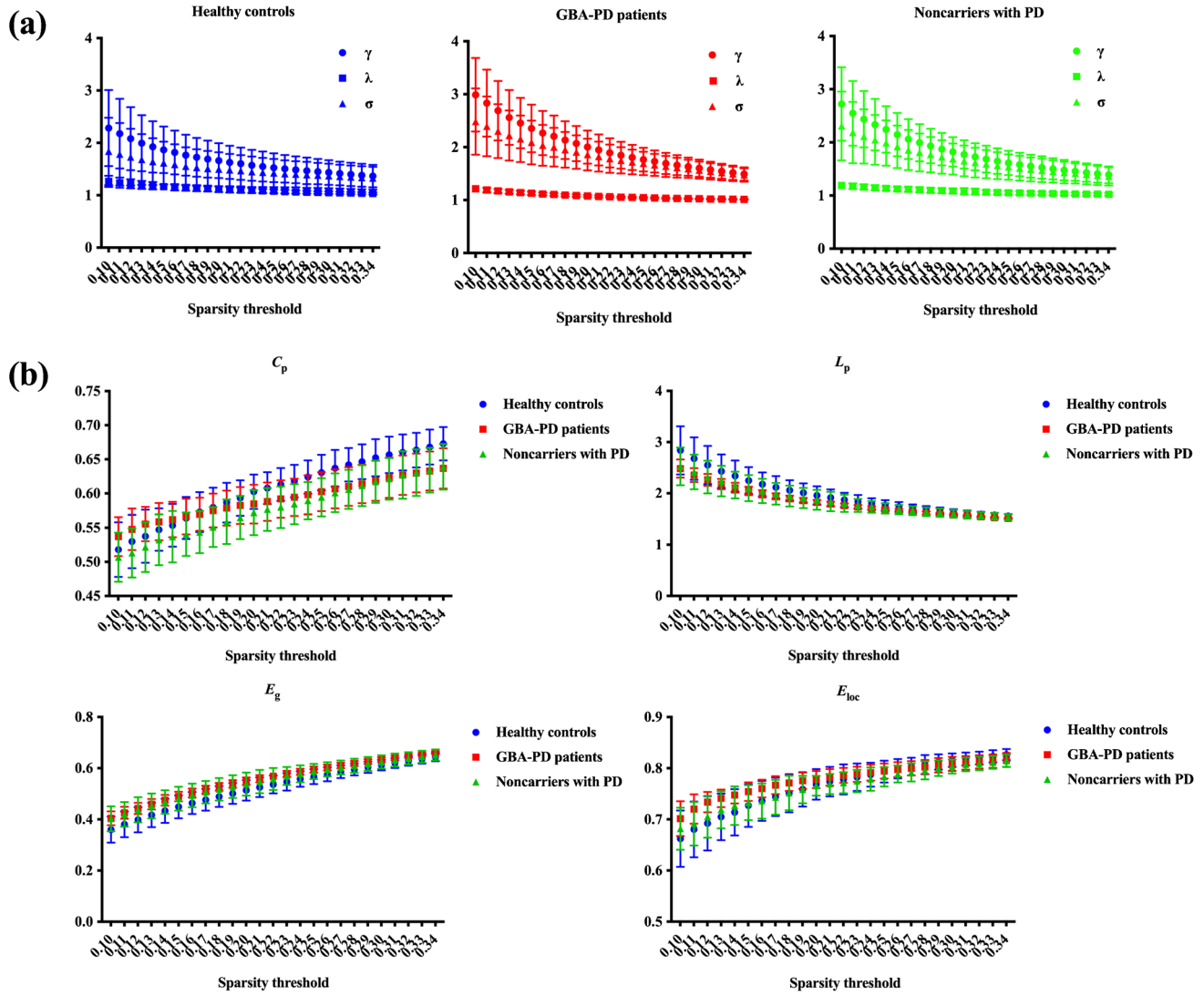

Fig. 1 (**a**) Small-world properties among the three groups (the GBA-PD group, PD noncarrier group, and healthy controls); (**b**) Global topological properties of functional networks among the three groups over the selected range of the sparsity threshold. Abbreviations: C_p clustering coefficient, E_g global efficiency, E_{loc} local efficiency, *GBA* glucocerebrosidase gene, L_p characteristic path length, *PD* Parkinson's disease

and HCs showed global parameters over the selected range of the sparsity threshold (Fig. 1b). Statistical comparisons (ANOVA with LSD post hoc test) were performed to detect significant differences in global properties among the three groups. Compared to HCs, the GBA-PD group showed a significantly decreased characteristic path length ($p = 0.018$) and a significantly increased global efficiency ($p = 0.010$); the noncarrier group showed a significantly decreased clustering coefficient ($p = 0.004$). No significant difference was found in the local efficiency among the three groups. Moreover, no significant difference was found in any global properties between the two PD subgroups, but showing an interesting trend (L_p: GBA-PD patients < noncarriers with PD < HCs; E_g: GBA-PD patients > PD noncarriers > HCs; C_p: noncarriers with PD < GBA-PD patients < HCs) (Table 2).

Eleven cerebral regions exhibiting significantly altered nodal betweenness centrality among the three groups were observed and mainly located in the default mode network (DMN), cingulo-opercular network, sensorimotor network (SMN), and occipital network. Using the LSD post hoc test, the GBA-PD group exhibited significantly increased nodal betweenness centrality in the medial prefrontal cortex (mPFC) and precuneus within the DMN, and precentral gyrus within the SMN, while decreased nodal betweenness centrality in the anterior insular and temporal region within the cingulo-opercular network compared to the noncarrier group. Compared to HCs, both PD subgroups exhibited

Table 2 Group comparisons of AUC values of global network properties

Group	C_p	L_p	E_g	E_{loc}
Healthy controls	0.146 ± 0.006	0.472 ± 0.040	0.126 ± 0.008	0.184 ± 0.007
GBA-PD patients	0.142 ± 0.006	0.439 ± 0.013	0.134 ± 0.003	0.187 ± 0.003
Noncarriers with PD	0.139 ± 0.007	0.448 ± 0.040	0.132 ± 0.009	0.184 ± 0.005
p-value (ANOVA)	**0.014***	**0.042***	**0.022***	0.310
p-value (healthy controls vs. GBA-PD patients)	0.110	**0.018***	**0.010***	0.212
p-value (healthy controls vs. noncarriers with PD)	**0.004***	0.085	0.053	0.732
p-value (GBA-PD patients vs. noncarriers with PD)	0.214	0.528	0.519	0.155

ANOVA analysis of variance, *AUC* area under the curve, C_p clustering coefficient, E_g global efficiency E_{loc} local efficiency *GBA* glucocerebrosidase gene, L_p characteristic path length, *PD* Parkinson's disease

*$p < 0.05$ (ANOVA, LSD post hoc test)

significantly decreased nodal betweenness centrality in the angular gyrus and intraparietal sulcus within the DMN, and temporal region within the occipital network. In addition, the GBA-PD group exhibited significantly increased nodal betweenness centrality in the mPFC, precuneus, and occipital region within the DMN, and precentral gyrus within the SMN, while decreased nodal betweenness centrality in the parietal region within the SMN compared to HCs. The noncarrier group exhibited significantly increased nodal betweenness centrality in the anterior and middle insular and temporal regions within the cingulo-opercular network compared to HCs (Table 3, Fig. 2).

Correlation analysis

By performing partial correlation analysis, we found that the nodal betweenness centrality of mPFC showed a significantly positive correlation with the fatigue severity scale scores ($r = 0.571$, $p = 0.017$) in all patients with PD. In addition, we did not find any significant correlation between the remaining regional betweenness centralities and clinical features in patients with PD.

Discussion

The current study is, to our knowledge, the first to apply the graph theory to observe the disruption of the topological organization of functional brain networks in GBA-PD patients. Our major findings revealed the following: (1) the GBA-PD group showed prominently decreased characteristic path length and increased global efficiency compared to HCs at the global level; (2) although both PD groups

Table 3 Abnormal nodal betweenness centrality among the three groups for functional networks

		Betweenness centrality			*p*-value (post hoc)			
Networks	Regions	Healthy controls	GBA-PD patients	Noncarriers with PD	*p*-value (ANOVA)	Healthy controls vs. GBA-PD patients	Healthy controls vs. noncarriers with PD	GBA-PD patients vs. noncarriers with PD
DMN	mPFC	13.30 ± 8.12	30.18 ± 19.97	15.91 ± 9.78	0.004	**0.001***	0.597	**0.013***
DMN	precuneus	11.15 ± 7.95	22.98 ± 18.92	8.74 ± 5.12	0.012	**0.011***	0.588	**0.006***
DMN	angular gyrus	32.51 ± 15.97	16.69 ± 12.72	19.33 ± 12.38	0.010	**0.006***	**0.021***	0.665
DMN	IPS	40.06 ± 28.83	18.56 ± 8.01	22.39 ± 15.16	0.023	**0.013***	**0.038***	0.678
DMN	occipital	16.22 ± 12.57	32.66 ± 17.36	23.75 ± 19.94	0.039	**0.012***	0.231	0.204
CON	ant insula	19.75 ± 10.35	24.96 ± 15.44	41.96 ± 23.90	0.004	0.411	**0.001***	**0.020***
CON	mid insula	8.30 ± 6.07	13.23 ± 12.01	22.15 ± 22.54	0.044	0.360	**0.013***	0.141
CON	temporal	21.60 ± 22.87	12.72 ± 8.48	42.14 ± 33.30	0.017	0.333	**0.029***	**0.006***
SMN	precentral gyrus	16.87 ± 13.10	32.47 ± 22.34	17.75 ± 13.23	0.038	**0.016***	0.888	**0.039***
SMN	parietal	29.67 ± 26.20	11.70 ± 8.25	16.54 ± 9.43	0.040	**0.018***	0.078	0.552
Occipital	occipital	53.62 ± 39.90	27.83 ± 23.18	26.57 ± 12.92	0.033	**0.033***	**0.025***	0.923

ANOVA analysis of variance, *ant* antieror, *CON* cingulo-opercular network, *DMN* default mode network, *GBA* glucocerebrosidase gene, *IPS* intraparietal sulcus, *mid* middle, *mPFC* medial prefrontal cortex, *PD* Parkinson's disease, *SMN* sensorimotor network

*$p < 0.05$ (ANOVA, LSD post hoc test)

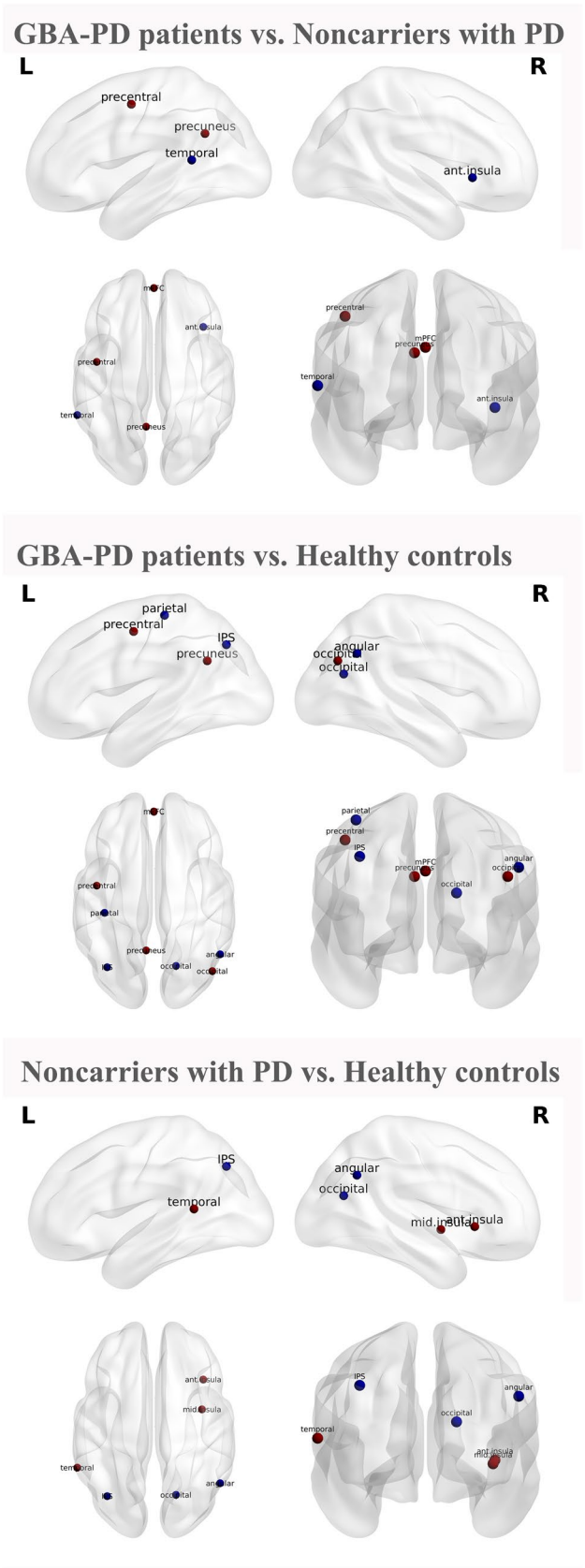

Fig. 2 The differences in nodal betweenness centrality of the functional networks among the three groups (the GBA-PD group, PD noncarrier group, and healthy controls). The disrupted nodes with significantly decreased or increased betweenness centrality are shown in blue or red. Abbreviations: *ant* anterior, *GBA* glucocerebrosidase gene, *IPS* intraparietal sulcus, *mid* middle, *mPFC* medial prefrontal cortex, *PD*, Parkinson's disease

showed a significant decline of betweenness centrality in nodes within the DMN and occipital network, the GBA-PD group showed a significantly increased nodal betweenness centrality in the mPFC, precuneus, and precentral gyrus, while a significantly decreased betweenness centrality in nodes within the cingulo-opercular network compared to the noncarrier group at the regional level; (3) the altered nodal betweenness centrality of mPFC was significantly correlated with fatigue severity scale scores of patients with PD, indicating a potential biomarker of fatigue in PD.

The human brain is characterized as a small-world network with a balance between the high clustering coefficient (functional segregation) and low characteristic path length (functional integration) [19], which is responsible for efficient local information processing and efficient long-distance connectivity. Meantime, high global efficiency as the superior measure of integration may significantly contribute to integration in networks. In the present study, the functional brain networks of GBA-PD patients exhibited the lower characteristic path length and higher global efficiency, indicating increased information transfer between long-range connectivity (functional integration). The functional brain networks of noncarriers with PD exhibited the lower clustering coefficient, indicating decreased local information processing (functional segregation), suggesting a shift of the optimal topological organization of functional networks in patients with PD. Several rs-fMRI studies also exhibited disrupted topological organization of functional networks in patients with PD when compared to HCs [11, 20, 21]. Luo et al. found no significant difference in global efficiency but reduced local efficiency [11]; while Sreenivasan et al. found reduced global and local efficiency in early-stage drug-naïve patients with PD [20]. Moreover, Suo et al. found decreased global and local efficiency in patients with PD with different H&Y stages [21]. The discrepancy in the disease stage might affect the difference of topological network organization, and the distinct topological organization may be a result of different pathophysiology in the inherently heterogeneous disease.

In addition to the overall network metrics, several nodes showed significantly altered betweenness centrality characteristics both in GBA-PD patients and noncarriers with PD in our cohort, which spatially overlapped with the pathological process-related specific regions, including initial mesocortex, progressing to high-order sensory association and

prefrontal areas, and eventually affecting premotor as well as primary sensory/motor fields [22]. A significant decline of nodal betweenness centrality within the DMN and the occipital network was found in both PD groups compared to HCs, which may be compatible with the roles for dysfunctional connectivity of DMN in cognitive decline and of the occipital network in impaired visual processing in patients with PD [23, 24].

Of note, in the present study, we found a significantly increased nodal betweenness centrality in the mPFC and precuneus in GBA-PD patients compared to noncarriers with PD. The mPFC, as a crucial cortical region that can integrate information from cortical/subcortical regions and converge information to output structures, plays essential roles in the motivation, cognitive process, regulation of emotion, and sociability [25]. The precuneus also plays a central role in a wide spectrum of highly integrated tasks, including visuo-spatial imagery, episodic memory retrieval, and self-processing operations [26]. In PD, the mPFC and precuneus and their connected regions have been reported to be associated with the pathophysiology of non-motor symptoms [27]. We thus assumed that the alteration of functional connections located in these regions might be closely related to non-motor symptoms of PD. It has only recently been recognized that fatigue is a common problem in PD, and the neural bases of fatigue in PD remain uncertain [28]. Fatigue in diseases of the central nervous system has recently been reported to be associated with dysfunction of basal ganglia (BG) [29]. Moreover, fatigue was found to be associated with reduced glucose metabolism in the BG and frontal cortex in patients with multiple sclerosis [30]. Prior models of fatigue in neurologic diseases proposed the dysfunction of the BG and medial frontal cortex to generate fatigue. Deep brain stimulation of subthalamic regions structurally connected with the frontal cortex was found to be associated with autonomous effects such as tiredness/fatigue [31]. Interestingly, we also revealed the altered nodal betweenness centrality in the mPFC was positively correlated with clinical fatigue severity in patients with PD. The GBA-PD group even presented significantly enhanced nodal betweenness centrality in the mPFC, relatively higher fatigue severity scale scores, and more patients with fatigue compared to the noncarrier group, which lending credence to the pathophysiologic relevance of fatigue in PD.

In addtion, we found that GBA-PD patients showed significantly increased nodal betweenness centrality in the precentral gyrus compared to noncarriers with PD, and the nodal betweenness centrality of the latter is similar to that of HCs. The classic motor impairment of PD might be in accordance with the decreased nodal centralities in the sensorimotor cortex [21], but we did not find this change in our two PD subgroups. Although medication was withdrawn at least 12 h in treated patients with PD before the MRI scanning, the potentially confounding effects of chronic dopaminergic drugs may not be explicitly ruled out. Possible explanations of the difference may be the heterogeneity of patients with PD, and we conjectured that the enhanced function in the precentral gyrus might be a compensatory response, which might be more remarkable in GBA-PD patients. We also revealed that GBA-PD patients showed significantly decreased nodal betweenness centrality within the cingulo-opercular network compared to noncarriers with PD, and the nodal betweenness centrality of the former is similar to that of HCs. The cingulo-opercular network that is primarily composed of the anterior insula and dorsal anterior cingulate cortex has generally been equated with the salience network [32], which is associated with the detection and integration of emotional and sensory stimuli, and modulation of the switch of cognition between the DMN and central executive network. We thus speculated that GBA-PD patients may lack this compensatory function within the cingulo-opercular network compared to noncarriers with PD. Future studies in larger patient populations are warranted to clarify these views.

The mechanism underlying the association between GBA mutations and PD is still unclear. Although our GBA-PD patients and noncarriers with PD presented minor clinical differences, the neuroimaging technique highlighted the interesting effects of GBA mutations. Here, the altered nodal betweenness centrality was detected at a low threshold, because of the small number of GBA-PD patients ($n = 11$). These preliminary results may provide new clues for which pathways or networks may be altered in GBA-related PD. GBA-PD patients displayed altered nodal betweenness centrality mainly within the DMN, corroborating the clinical findings that patients with PD with GBA mutations carry a higher risk of non-motor symptoms, especially the cognitive impairment [33]. The notable finding of impaired nodal betweenness centrality in the mPFC associated with fatigue in PD may provide evidence in support of a serotonergic pathway in patients with fatigue [34], and reflect the greater progression of the GBA-PD group on fatigue, despite the absence of difference in fatigue severity scale scores with the noncarrier group. The discovery of this imaging evolution before prominent clinical manifestations is crucial not only for its prognosis but also for elucidating the pathophysiology of the disease.

Several limitations needed to be addressed. First, the current study had a cross-sectional design and was a preliminary pilot study, as only 11 patients in each PD subgroup; therefore, our findings did not take into account the heterogeneity of the GBA mutations, even though these mutations were defined as pathological/likely pathological variations, which should be interpreted with caution. Second, the topological organization of brain networks has been proven to be affected by the different parcellation

strategies [35], although the templates used in this study have been widely used to construct human brain organization. Third, although the drug usage was controlled between the two PD subgroups and withdrawn at least 12 h in the study, the comparison between patients with PD and HCs could still be affected by drug usage. Further studies are warranted to evaluate the effect of the medication on the topologic properties of brain networks in GBA-PD patients.

Conclusion

In the current study, graph theory analysis was used to investigate the altered topological organization in patients with PD with GBA mutations. GBA-PD patients showed the higher functional integration at the global level, and alterations of regions within the DMN, cingulo-opercular network, SMN, and occipital network at the nodal level. The finding of nodal betweenness centrality in the mPFC is congruent with the potential fatigue pathology in PD and suggestive of a profound effect of GBA mutations on the clinical fatigue in patients with PD. These results may extend the understanding of relationships between disruptions of functional networks and GBA-related pathophysiology in PD.

Supplementary Information The online version contains supplementary material available at https://doi.org/10.1007/s00234-022-03067-9.

Acknowledgements The authors thank the patients and their families for their participation in the study.

Author contribution Yanbing Hou: conception and design of the study, statistical analysis, interpretation of data, and drafting of manuscript
Fei Feng: data collection and statistical analysis
Lingyu Zhang: data collection and statistical analysis
Ruwei Ou: data collection
Junyu Lin: data collection
Qiyong Gong: study design, analysis and interpretation, and revision of the manuscript
Huifang Shang: study design, analysis and interpretation, and revision of the manuscript

Funding The present study was supported by the National Key Research and Development Program of China (Grant No. 2021YFC2501203 to FHS); and the Sichuan Science and Technology Program (Grant No. 2022ZDZX0023 to FHS).

Data availability The data that support the findings of this study are available on request from the corresponding author. The data are not publicly available due to privacy or ethical restrictions.

Declarations

Conflict of interest The authors declare no competing interests.

Ethics approval Approval was received from the West China Hospital of Sichuan University Clinical trials and Biomedical ethics committee.

Consent to participate Written informed consent was obtained from all participants in the study.

References

1. Bloem BR, Okun MS, Klein C (2021) Parkinson's disease. Lancet 397:2284–2303. https://doi.org/10.1016/S0140-6736(21)00218-X
2. Sidransky E, Nalls MA, Aasly JO et al (2009) Multicenter analysis of glucocerebrosidase mutations in Parkinson's disease. N Engl J Med 361:1651–1661. https://doi.org/10.1056/NEJMoa0901281
3. Balestrino R, Schapira AHV (2018) Glucocerebrosidase and Parkinson disease: molecular, clinical, and therapeutic implications. Neuroscientist 24:540–559. https://doi.org/10.1177/1073858417748875
4. Blandini F, Cilia R, Cerri S et al (2019) Glucocerebrosidase mutations and synucleinopathies: toward a model of precision medicine. Mov Disord 34:9–21. https://doi.org/10.1002/mds.27583
5. Saeed U, Lang AE, Masellis M (2020) Neuroimaging advances in Parkinson's disease and atypical Parkinsonian syndromes. Front Neurol 11:572976. https://doi.org/10.3389/fneur.2020.572976
6. Filippi M, Balestrino R, Basaia S, Agosta F (2022) Neuroimaging in glucocerebrosidase-associated Parkinsonism: a systematic review. Mov Disord 37:1375–1393. https://doi.org/10.1002/mds.29047
7. Leocadi M, Canu E, Donzuso G et al (2022) Longitudinal clinical, cognitive, and neuroanatomical changes over 5 years in GBA-positive Parkinson's disease patients. J Neurol 269:1485–1500. https://doi.org/10.1007/s00415-021-10713-4
8. Agosta F, Kostic VS, Davidovic K et al (2013) White matter abnormalities in Parkinson's disease patients with glucocerebrosidase gene mutations. Mov Disord 28:772–778. https://doi.org/10.1002/mds.25397
9. Thaler A (2018) Structural and functional MRI in familial Parkinson's disease. Int Rev Neurobiol 142:261–287. https://doi.org/10.1016/bs.irn.2018.09.005
10. Greuel A, Trezzi JP, Glaab E et al (2020) GBA Variants in Parkinson's disease: clinical, metabolomic, and multimodal neuroimaging phenotypes. Mov Disord 35:2201–2210. https://doi.org/10.1002/mds.28225
11. Luo CY, Guo XY, Song W et al (2015) Functional connectome assessed using graph theory in drug-naive Parkinson's disease. J Neurol 262:1557–1567. https://doi.org/10.1007/s00415-015-7750-3
12. Hughes AJ, Daniel SE, Kilford L, Lees AJ (1992) Accuracy of clinical diagnosis of idiopathic Parkinson's disease: a clinico-pathological study of 100 cases. J Neurol Neurosurg Psychiatry 55:181–184
13. Emre M, Aarsland D, Brown R et al (2007) Clinical diagnostic criteria for dementia associated with Parkinson's disease. Mov Disord 22:1689–1707. https://doi.org/10.1002/mds.21507 (**quiz 1837**)
14. Tomlinson CL, Stowe R, Patel S, Rick C, Gray R, Clarke CE (2010) Systematic review of levodopa dose equivalency reporting in Parkinson's disease. Mov Disord 25:2649–2653. https://doi.org/10.1002/mds.23429
15. Power JD, Barnes KA, Snyder AZ, Schlaggar BL, Petersen SE (2012) Spurious but systematic correlations in functional connectivity MRI networks arise from subject motion. Neuroimage 59:2142–2154. https://doi.org/10.1016/j.neuroimage.2011.10.018
16. Hou Y, Wei Q, Ou R, Yang J, Gong Q, Shang H (2020) Impaired topographic organization in Parkinson's disease with mild cognitive impairment. J Neurol Sci 414:116861. https://doi.org/10.1016/j.jns.2020.116861

17. Medaglia JD (2017) Graph Theoretic analysis of resting state functional MR imaging. Neuroimaging Clin N Am 27:593–607. https://doi.org/10.1016/j.nic.2017.06.008
18. Dosenbach NU, Nardos B, Cohen AL et al (2010) Prediction of individual brain maturity using fMRI. Science 329:1358–1361. https://doi.org/10.1126/science.1194144
19. Rubinov M, Sporns O (2010) Complex network measures of brain connectivity: uses and interpretations. Neuroimage 52:1059–1069. https://doi.org/10.1016/j.neuroimage.2009.10.003
20. Sreenivasan K, Mishra V, Bird C et al (2019) Altered functional network topology correlates with clinical measures in very early-stage, drug-naive Parkinson's disease. Parkinsonism Relat Disord 62:3–9. https://doi.org/10.1016/j.parkreldis.2019.02.001
21. Suo X, Lei D, Li N et al (2017) Functional brain connectome and its relation to Hoehn and Yahr stage in Parkinson disease. Radiology 285:904–913. https://doi.org/10.1148/radiol.2017162929
22. Braak H, Del Tredici K, Rub U, de Vos RA, Jansen Steur EN, Braak E (2003) Staging of brain pathology related to sporadic Parkinson's disease. Neurobiol Aging 24:197–211. https://doi.org/10.1016/s0197-4580(02)00065-9
23. Meppelink AM, de Jong BM, Renken R, Leenders KL, Cornelissen FW, van Laar T (2009) Impaired visual processing preceding image recognition in Parkinson's disease patients with visual hallucinations. Brain 132:2980–2993. https://doi.org/10.1093/brain/awp223
24. Raichle ME, MacLeod AM, Snyder AZ, Powers WJ, Gusnard DA, Shulman GL (2001) A default mode of brain function. Proc Natl Acad Sci U S A 98:676–682. https://doi.org/10.1073/pnas.98.2.676
25. Xu P, Chen A, Li Y, Xing X, Lu H (2019) Medial prefrontal cortex in neurological diseases. Physiol Genomics 51:432–442. https://doi.org/10.1152/physiolgenomics.00006.2019
26. Cavanna AE, Trimble MR (2006) The precuneus: a review of its functional anatomy and behavioural correlates. Brain 129:564–583. https://doi.org/10.1093/brain/awl004
27. Ramos BP, Arnsten AF (2007) Adrenergic pharmacology and cognition: focus on the prefrontal cortex. Pharmacol Ther 113:523–536. https://doi.org/10.1016/j.pharmthera.2006.11.006
28. Friedman JH, Brown RG, Comella C et al (2007) Fatigue in Parkinson's disease: a review. Mov Disord 22:297–308. https://doi.org/10.1002/mds.21240
29. Chaudhuri A, Behan PO (2004) Fatigue in neurological disorders. Lancet 363:978–988. https://doi.org/10.1016/S0140-6736(04)15794-2
30. Roelcke U, Kappos L, Lechner-Scott J et al (1997) Reduced glucose metabolism in the frontal cortex and basal ganglia of multiple sclerosis patients with fatigue: a 18F-fluorodeoxyglucose positron emission tomography study. Neurology 48:1566–1571. https://doi.org/10.1212/wnl.48.6.1566
31. Strotzer QD, Kohl Z, Anthofer JM et al (2022) Structural connectivity patterns of side effects induced by subthalamic deep brain stimulation for Parkinson's disease. Brain Connect 12:374–384. https://doi.org/10.1089/brain.2021.0051
32. Menon V, Uddin LQ (2010) Saliency, switching, attention and control: a network model of insula function. Brain Struct Funct 214:655–667. https://doi.org/10.1007/s00429-010-0262-0
33. Wolters AF, van de Weijer SCF, Leentjens AFG, Duits AA, Jacobs HIL, Kuijf ML (2019) Resting-state fMRI in Parkinson's disease patients with cognitive impairment: a meta-analysis. Parkinsonism Relat Disord 62:16–27. https://doi.org/10.1016/j.parkreldis.2018.12.016
34. Pavese N, Metta V, Bose SK, Chaudhuri KR, Brooks DJ (2010) Fatigue in Parkinson's disease is linked to striatal and limbic serotonergic dysfunction. Brain 133:3434–3443. https://doi.org/10.1093/brain/awq268
35. Wang J, Wang L, Zang Y et al (2009) Parcellation-dependent small-world brain functional networks: a resting-state fMRI study. Hum Brain Mapp 30:1511–1523. https://doi.org/10.1002/hbm.20623